Kinetics of the Self-Reaction of C_2H_5 Radicals

Eugene V. Shafir, Irene R. Slagle, and Vadim D. Knyazev*

Research Center for Chemical Kinetics, Department of Chemistry, The Catholic University of America, Washington, D.C. 20064

Received: April 3, 2003; In Final Form: June 27, 2003

The kinetics of the self-reaction of ethyl radicals was studied by laser photolysis/photoionization mass spectroscopy. Overall rate constants were obtained in direct real-time experiments in the temperature region 301−800 K and at bath gas (mostly helium, balance radical precursors) densities of (3.00−12.0) × 10^{16} molecules cm^{-3}. Ethyl radicals were produced in well-characterized concentrations by a combination of the 193-nm photolysis of oxalyl chloride ($(CClO)_2$) with the subsequent fast reaction of Cl atoms with ethane. The observed overall $C_2H_5 + C_2H_5$ rate constants demonstrate a negative temperature dependence. Master equation modeling of collisional effects indicates that the reaction is in the high-pressure limit under all experimental conditions except for those used at the highest temperature, 800 K, where a minor falloff correction (8%) was applied to obtain the high-pressure-limit rate constant value. The following expression for the high-pressure-limit rate constant of reaction 1 was obtained: $k_1^\infty = (2.29 \times 10^{-6})\, T^{-1.66} \exp(-552\ \mathrm{K}/T)$ cm^3 $molecule^{-1}$ s^{-1}. The disproportionation to recombination branching ratio was determined at 297 and 400 K; the results are in agreement with the well-established value of 0.14.

I. Introduction

Radical−radical reactions are important elementary steps in the combustion and pyrolysis of hydrocarbons.[1,2] These reactions generally, although not without exceptions, serve as chain termination pathways. Despite their importance, information available on the rates of these reactions is sparse and often controversial, as radical−radical reactions are difficult to study experimentally due to the high reactivity of the species involved.

The ethyl radical self-reaction is an important elementary step leading to termination of chain reactions in oxidation and pyrolysis of hydrocarbons. Knowledge of the rate constant and the channel branching ratio of this reaction is necessary for accurate modeling of the combustion of organic fuels. In addition, this reaction has been used as a reference reaction in numerous experimental studies based on final product analysis, where rates of other elementary gas-phase reactions were derived relative to that of the ethyl radical self-reaction. To obtain absolute rate constant values from the results of these relative rates studies, accurate knowledge of the rate constant of the ethyl radical self-reaction is needed.

The C_2H_5 self-reaction,

$$C_2H_5 + C_2H_5 \rightarrow C_4H_{10} \qquad (1a)$$

$$\rightarrow C_2H_4 + C_2H_6 \qquad (1b)$$

has been studied extensively over the past 40 years by various experimental methods. Reviews of these studies can be found, for example, in refs 1, 3, and 4. In 1957, Shepp and Kutschke[5] used the photolysis of diethyl ketone as a source of ethyl radicals in combination with the rotating sector technique to determine the rate constant of reaction 1. Experimental studies gained a new impetus with the development of molecular modulation spectroscopy. Parkes and Quinn,[6] Arthur,[7] and Anastasi and Arthur[8] applied this technique to determine the rate of the ethyl radical self-reaction. Their results relied on an assumed kinetic mechanism and knowledge of the UV absorption cross section of C_2H_5. Only two direct studies in which the kinetics of the C_2H_5 decay due to self-reaction was monitored in real-time experiments are reported in the literature.[9,10] Adachi and coworkers[9] used the flash photolysis of diazoethane and UV absorption spectroscopy to study reaction 1; Atkinson and Hudgens[10] used laser photolysis of Cl_2 with subsequent fast reaction of Cl atoms with ethane to produce C_2H_5 and laser cavity ring-down spectroscopy to detect ethyl radicals. Both of these studies used spectroscopic techniques to detect C_2H_5, and thus the results were dependent on the UV absorption cross sections of C_2H_5, which were determined in separate experiments.

Only the experiments of Arthur[7] included a study of reaction 1 over a small temperature interval (300−373 K); all other studies were conducted at room temperature. The room-temperature values of the rate constant of the C_2H_5 self-reaction obtained in refs 6−10 range from 1.5 × 10^{-11} to 2.3 × 10^{-11} cm^3 $molecule^{-1}$ s^{-1}.

In this work, we present the results of the first direct real-time temperature-dependent experimental investigation of the self-reaction of ethyl radicals. Reaction 1 was studied by laser photolysis/photoionization mass spectrometry. A relatively novel approach based on the method developed by Baklanov and Krasnoperov[11,12] was used to photolytically produce ethyl radicals in known concentrations: 193-nm laser photolysis of oxalyl chloride ($(CClO)_2$), producing Cl atoms, followed by a fast reaction of Cl with ethane. The experimental method was first validated by determining the rate constants of the well-studied reaction of recombination of methyl radicals. Overall rate constants of reaction 1 were obtained in the temperature interval 301−800 K and bath gas (mostly helium, balance radical precursors) densities in the range (3.00−12.0) × 10^{16} molecules cm^{-3}. The branching ratio of channels 1a and 1b was

* Corresponding author. E-mail: knyazev@cua.edu.

10.1021/jp034876e CCC: $25.00
Published on Web 08/07/2003

obtained at low temperatures (297−400K) and a bath gas density of 12.0×10^{16} molecules cm^{-3}.

This article is organized as follows. Section I is an introduction. Section II presents the experimental methods used for determination of the rate constants and the branching ratio. Experimental results are described in section III. Finally, a discussion is presented in section IV.

II. Experimental Section

In this section, a description of the experimental apparatus and the photolytic sources of radicals is first presented. A description of the method of determination of the rate constants is then given, followed by that of the method of determining the disproportionation to recombination branching ratio.

Apparatus. Details of the experimental apparatus have been described previously;[13] only a brief description is given here. Pulsed 193-nm unfocused light from a Lambda Physik 201 MSC excimer laser was directed along the axis of a heated 50-cm-long tubular reactor (i.d. 1.05 cm). The reactor surface was coated with halocarbon wax, poly(dimethylsiloxane),[14] or boron oxide.[14] The laser was operated at 4 Hz and a fluence of 40−250 mJ/pulse.

To replace the photolyzed gas mixture with fresh reactants between laser pulses, the flow of the gas mixture containing the radical precursors and the bath gas (helium) was set at ∼4 m s^{-1}. The mixture was continuously sampled through a small tapered orifice in the wall of the reactor and formed into a beam by a conical skimmer before entering the vacuum chamber containing the photoionization mass spectrometer. As the gas beam traversed the ion source, a portion was photoionized by an atomic resonance lamp, mass-selected by a quadrupole mass filter, and detected by a Daly detector. Temporal ion signal profiles were recorded from a short time before the laser pulse (10−30 ms) to 15−30 ms following the pulse by a multichannel scaler interfaced to a personal computer. Typically, data from 1000−15000 repetitions of the experiment were accumulated before the data were analyzed. The sources of the photoionization radiation were chlorine (8.9−9.1 eV, CaF_2 window, used to detect C_2H_5), hydrogen (10.2 eV, MgF_2 window, used to detect CH_3, $(CH_3)_2CO$, and $(C_2H_5)_2CO$), and argon (11.6−11.9 eV, LiF window, used to detect $(CClO)_2$, C_2H_4, C_3H_8, and C_4H_{10}) resonance lamps.

Radical Precursors. Real-time experimental studies of radical self-reactions, ideally, require a suitable pulsed source of radicals that should satisfy two requirements: (1) the radicals of interest are the only reactive species present in the reactor during the kinetics of radical decay, and (2) the initial concentration of radicals can be determined with a high degree of accuracy.

Recently, Baklanov and Krasnoperov[11] suggested using the 193-nm photolysis of oxalyl chloride ($(CClO)_2$) with conversion of Cl atoms produced to the radicals of interest (R) by a fast reaction with a suitable substrate:

$$(CClO)_2 \xrightarrow{193\ nm} 2Cl + 2CO \quad (2a)$$

$$\rightarrow Cl + CO + CClO \rightarrow 2Cl + 2CO \quad (2b)$$

$$Cl + RH \rightarrow R + HCl \quad (3)$$

The CClO radical has a high thermal decomposition rate, even at room temperature (e.g., $k > 600\ s^{-1}$ at the pressures used in the current study).[15] Thus, the 193-nm photolysis of oxalyl chloride can serve as a "clean" photolytic source of chlorine atoms ("clean" in the sense that no other reactive species are produced by the photolysis). Since the yield of chlorine atoms in reaction 2 is exactly 200%, the initial concentration of Cl (and, consequently, that of R) can be determined from the extent of the photolytic depletion of oxalyl chloride, which, in turn, can be measured spectroscopically[11,12] or mass spectrometrically. Recently, Baklanov and Krasnoperov applied this method of pulsed generation of radicals to study the self-reaction of silyl radicals.[12]

In the current study, the 193-nm photolysis of $(CClO)_2$ with subsequent fast reaction of the Cl atoms with ethane or methane was used as a source of ethyl and methyl radicals. Concentrations of RH (ethane or methane) were selected to ensure a virtually instantaneous (on the time scale of the reactions studied) conversion of Cl into the radicals of interest (C_2H_5 or CH_3).

A separate set of experiments was carried out to verify the validity of the technique of kinetic studies based on the described method of radical generation (see section III). The rate constant of the methyl radical recombination was determined at 577 K and bath gas densities of (8 and 12.0) $\times 10^{16}$ molecules cm^{-3} using two different photolytic sources of CH_3. In the first source, the reaction between chlorine atoms (produced in the photolysis of oxalyl chloride, reaction 2) and methane was used to generate methyl radicals. The 193-nm photolysis of acetone was employed as the second radical source:

$$(CH_3)_2CO \rightarrow 2CH_3 + CO \quad (4)$$

Reaction 4 is known to account for more than 95% of the products of acetone photolysis.[16] This second source of methyl radicals was used earlier by Slagle et al.[17] in an experimental study of the recombination of methyl radicals. Comparison of the rate constant values obtained in the current work using the two different photolytic sources of CH_3 with each other and with those of ref 17 serves to validate the approach based on the use of reactions 2 and 3 as a source of radicals (see section III).

In yet another separate set of experiments, the 193-nm photolysis of diethyl ketone was used as a source of ethyl radicals:

$$(C_2H_5)_2CO \rightarrow 2C_2H_5 + CO \quad (5a)$$

$$\rightarrow \text{other products} \quad (5b)$$

By analogy with the photolysis of acetone,[16] one can expect the ethyl radicals and CO to be the main product channel of the $(C_2H_5)_2CO$ photolysis. In fact, on the basis of this assumption, $(C_2H_5)_2CO$ photolysis was used as a photolytic source of C_2H_5 in a number of earlier studies of the C_2H_5 self-reaction.[3] Our results (section III) demonstrate that, while channel 5a appears to be dominant at room temperature, at higher temperatures significant amounts of species other than the ethyl radical are produced.

Method of Determination of Rate Constants. The radicals (C_2H_5 or CH_3) were produced by the 193-nm photolysis of the corresponding precursors (or mixtures of precursors) diluted in the helium carrier gas. The kinetics of the radical decay was monitored in real time. The rate constant measurements were performed using a technique analogous to that applied by Slagle and co-workers to the study of the $CH_3 + CH_3$ reaction.[17] When the combination of reactions 2 and 3 was used as the source of radicals, experimental conditions were selected in such a way as to achieve the following:

(a) More than 99% of the chlorine atoms produced by the photolysis of oxalyl chloride reacted with the corresponding

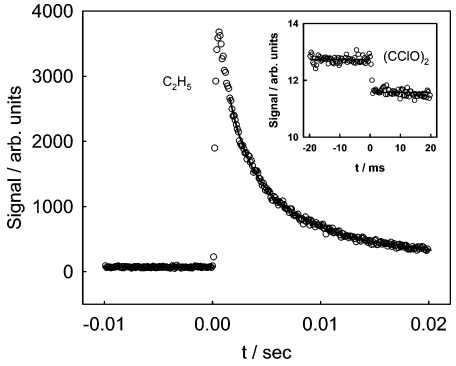

Figure 1. Typical temporal ion signal profiles recorded in an experiment to determine the rate of the $C_2H_5 + C_2H_5$ reaction. $T = 600$ K, [He] $= 12.0 \times 10^{16}$, $[C_2H_6] = 4.43 \times 10^{14}$, $[(CClO)_2] = 7.97 \times 10^{13}$, and $[C_2H_5]_0 = 1.59 \times 10^{13}$ molecules cm^{-3}. The solid curve on the main plot represents a fit of the experimental data with the kinetic mechanism consisting of reactions 1 and 6. The inset shows the decrease in the signal of oxalyl chloride due to photolytic depletion.

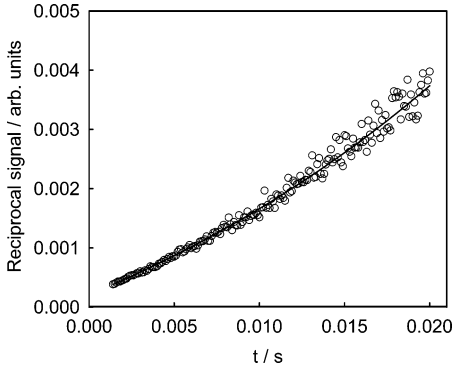

Figure 2. Reciprocal of the ion signal of C_2H_5 as a function of time. Conditions as in Figure 1. The solid curve represents a fit of the experimental data with the kinetic mechanism consisting of reactions 1 and 6.

hydrocarbon. To achieve this, the concentration of hydrocarbon was held such that the rate of the heterogeneous wall loss of chlorine atoms was less than 1% of the rate of the reaction between Cl and the corresponding hydrocarbon.

(b) The characteristic time of the reaction between Cl and hydrocarbon[18,19] was at least 20 times shorter (typically, 100−1000 times shorter) than that of the self-reaction of the radicals under study.

Under these experimental conditions, the self-reaction of the radicals of interest was unperturbed by any side process, and the only additional sink of the radicals was due to the heterogeneous wall loss, which was taken into account in the analysis. Thus, the experimental kinetic mechanism included reactions

$$C_2H_5 + C_2H_5 \rightarrow \text{products} \quad (1)$$

$$C_2H_5 \rightarrow \text{wall loss} \quad (6)$$

for the experiments on the self-reaction of ethyl radicals and

$$CH_3 + CH_3 (+M) \rightarrow C_2H_6(+M) \quad (7)$$

$$CH_3 \rightarrow \text{wall loss} \quad (8)$$

for the experiments on methyl radical recombination.

For this kinetic mechanism and the initial conditions described above, the corresponding first-order differential equations can be solved analytically:

$$S = \frac{S_0 k_w}{(2k' + k_w)\, e^{k_w t} - 2k'} \quad (I)$$

Here, $k' = k_r[R]_0$, where k_r is the self-reaction rate constant ($r = 1$ or 7) and $[R]_0$ is the initial radical concentration, S is the radical ion signal, S_0 is the initial signal amplitude, and k_w is the rate of the heterogeneous loss reaction (6 or 8). In each experiment, the values of the initial signal amplitude S_0, the wall loss rate k_w, and the $k_r[R]_0$ product were obtained from fits of the real-time radical decay profile. Typical signal profiles of oxalyl chloride and ethyl radical decay are shown in Figure 1. The line through the experimental S vs time profile was obtained from the fit of the data with eq I.

Different parts of the radical decay profiles exhibit different sensitivities to the fitting parameters. The initial part of the signal profile is most sensitive to the rate constant of the radical self-reaction, whereas the end part is most sensitive to the rate constant of the heterogeneous wall loss of radicals. These sensitivities are illustrated in Figure 2, where the reciprocal of the radical signal (with the baseline determined before the photolyzing laser pulse subtracted) is plotted as a function of time. In the absence of any heterogeneous wall loss of radicals (pure second-order decay), the reciprocal signal is directly proportional to time and forms a straight line; the self-reaction rate constant can be obtained from the slope of the line. In the presence of heterogeneous loss, the line is curved, the initial slope is proportional to $(2k' + k_w)$, and the deviation from a straight line can serve as a measure of the contribution from the heterogeneous wall loss. As can be seen from the plot in Figure 2, both the slope of the initial part of the reciprocal signal vs time dependence and the curvature are well characterized, which illustrates that both the $k_r[R]_0$ and k_w values can be obtained from the fit of the signal with a high degree of accuracy.

The rate of the heterogeneous loss of radicals (reactions 6 and 8) did not depend on the laser intensity or the concentration of the radical precursor, but it was affected by the condition of the walls of the reactor (such as coating material or history of exposure to different reacting mixtures). In principle, it was possible to obtain the values of k_6 and k_8 in separate experiments with low initial radical concentrations selected in such a way as to make the rates of radical self-reactions negligible. However, in experiments performed to determine the rates of radical self-reactions 1 and 7, a small fraction (<1%) of the Cl atoms produced in the photolysis of oxalyl chloride decayed on the reactor walls, which, together with the wall reaction of C_2H_5, could possibly have affected the wall conditions. Thus, it was more appropriate to determine the rates of wall losses of radicals in the same experiments for which the rates of radical self-reactions were obtained. Separate experiments with low radical concentrations (such that radical self-reactions were negligible) were performed periodically to confirm that the values of k_6 and k_8 obtained are in general agreement with those derived from the three-parameter fits of radical decays obtained with high radical concentrations.

When the combination of reactions 2 and 3 was used as a source of the radicals, the initial concentration of the radicals was determined by measuring the photolytic depletion of oxalyl chloride (the fraction of oxalyl chloride decomposed due to photolysis). The value of the decomposition ratio (the relative

decrease in radical precursor concentration upon photolysis) was obtained directly from the radical precursor ion profile (Figure 1). In the experiments in which photolysis of ketone (acetone or diethyl ketone) was used as the source of radicals, the initial concentration of the radicals was determined by measuring the photolytic depletion of the corresponding ketone. In each experiment to determine $k' = k_r[R]_0$, the decomposition ratio of oxalyl chloride or ketone was measured two times (before and after the kinetics of the radical decay was recorded).

For each experimental temperature, the initial radical concentration $[R]_0$ was varied by changing the concentration of oxalyl chloride or ketone and/or the laser fluence. The values of the $k_r[R]_0$ product obtained from the data fits were plotted as a function of the initial concentration of radicals obtained from the measurements of the photolytic depletion of the radical precursor ($[R]_0$). The values of the radical self-reaction rate constant were determined from the slopes of the linear $k_r[R]_0$ vs $[R]_0$ dependences.

Product Analysis. The self-reaction of ethyl radicals proceeds via two channels, those of recombination (1a) and disproportionation[4] (1b):

$$C_2H_5 + C_2H_5 \rightarrow C_4H_{10} \quad (1a)$$

$$\rightarrow C_2H_6 + C_2H_4 \quad (1b)$$

The experimental apparatus employed in this study is capable of real-time detection of the products of both channels. Such experiments, directed at determination of the disproportionation-to-recombination ratio, were performed at temperatures of 297 and 400 K. The recorded signals of butane (recombination channel, reaction 1a) and ethylene (disproportionation channel, reaction 1b) were numerically integrated, and the ratio of disproportionation to recombination rates was determined as the ratio of the signal integrals corrected for the ratio of sensitivities toward these species. The butane-to-ethylene sensitivity ratio was determined experimentally using known concentrations of these species.

The accuracy of the experiments to determine the disproportionation-to-combination ratio was limited by several factors: (1) the low sensitivity of the apparatus to ethylene, which further diminished in the presence of large concentrations of polyatomics (oxalyl chloride and ethane) in the reactor; (2) interfering ion signals at mass 28, resulting from ion fragmentation of butane and ethane; and (3) the necessity of performing experiments with very high concentrations of ethane so as to avoid even a minor contribution of the $Cl + C_2H_5 \rightarrow HCl + C_2H_4$ reaction[20] to the production of ethylene at very short reaction times. Since reaction channel 1b is minor ($\sim$12%[4]), the potential relative effect of the $Cl + C_2H_5$ reaction on the yield of C_2H_4 is larger by an order of magnitude than the potential effect of the same reaction on the initial concentration of C_2H_5, an effect which is negligible. Ion fragmentation contributions to the C_2H_4 signal were determined in separate experiments with only butane and ethane present in the reactor. The ion fragmentation of ethane significantly increased with temperature, and the resultant increase of the experimental uncertainty prevented determination of the branching ratio of channels 1a and 1b at temperatures above 400 K.

The sources of error in the measured experimental parameters, such as temperature, pressure, flow rate, signal count, etc., were subdivided into statistical and systematic errors and propagated to the final values of the rate constants and branching ratios using different mathematical procedures for propagating systematic and statistical uncertainties.[21] The error limits of the values reported in this work represent a sum of 2σ statistical uncertainty and estimated systematic uncertainty, unless specified otherwise.

TABLE 1: Conditions and Results of Experiments To Determine k_7 ($T = 577$ K)

[M][a]	precursor(s)		$[CH_3]_0$[d]	I[e]	$k_r[R]_0$[f]	k_w[g]
$k_7 = (1.88 \pm 0.18) \times 10^{-11}$ cm^3 molecule^{-1} s^{-1} at [M] = 8.0 [a]						
	$[CH_4]$[b]	**$[(CClO)_2]$**[c]				
8.0	3.69	4.73	0.74 ± 0.05	35	129 ± 5	4.8 ± 1.8
8.0	11.4	4.15	0.65 ± 0.06	35	127 ± 6	3.9 ± 1.9
8.0	3.74	9.35	1.57 ± 0.04	38	272 ± 12	0.0 ± 1.8
8.0	11.4	8.01	1.35 ± 0.04	38	233 ± 11	-1.6 ± 1.9
8.0	3.47	12.8	2.07 ± 0.16	37	417 ± 25	0.1 ± 2.0
8.0	18.4	9.82	1.59 ± 0.12	37	288 ± 15	2.8 ± 2.0
	$[(CH_3)_2CO]$[c]					
8.0		9.80	1.90 ± 0.06	36	352 ± 10	-2.9 ± 1.0
8.0		4.51	0.88 ± 0.03	36	188 ± 6	-3.4 ± 1.3
8.0		2.61	0.53 ± 0.02	36	129 ± 4	-4.7 ± 1.3
8.0		7.76	1.49 ± 0.03	36	278 ± 7	-3.4 ± 1.0
$k_7 = (2.14 \pm 0.28) \times 10^{-11}$ cm^3 molecule^{-1} s^{-1} at [M] = 12.0 [a]						
	$[CH_4]$[b]	**$[(CClO)_2]$**[c]				
12.0	2.83	8.40	1.34 ± 0.18	36	304 ± 17	-2.2 ± 2.1
12.0	21.9	8.40	1.34 ± 0.18	36	297 ± 23	1.3 ± 3.0
12.0	21.9	4.83	0.69 ± 0.01	32	178 ± 11	0.0 ± 2.8
12.0	21.9	4.70	0.66 ± 0.06	32	148 ± 6	2.2 ± 1.9
12.0	2.72	4.51	0.63 ± 0.05	32	128 ± 5	3.6 ± 1.6
	$[(CH_3)_2CO]$[c]					
12.0		8.45	1.6 ± 0.16	36	289 ± 8	-0.7 ± 1.0
12.0		6.98	1.23 ± 0.22	36	279 ± 8	-4.1 ± 1.2
12.0		8.37	1.40 ± 0.06	36	279 ± 10	-3.1 ± 1.4
12.0		3.33	0.55 ± 0.03	36	146 ± 6	-1.8 ± 1.9
12.0		3.43	0.54 ± 0.03	36	126 ± 6	-2.5 ± 2.2
12.0		9.06	1.36 ± 0.03	36	268 ± 9	-0.8 ± 1.4
12.0		4.96	0.92 ± 0.02	36	177 ± 4	-2.9 ± 1.0

[a] Concentration of the bath gas (mostly helium, balance radical precursors) in units of 10^{16} molecules cm^{-3}. [b] In units of 10^{15} molecules cm^{-3}. [c] In units of 10^{13} molecules cm^{-3}. [d] Nascent concentration of methyl radicals in units of 10^{13} molecules cm^{-3}, determined from the photolytic depletion of oxalyl chloride or acetone. [e] Estimated laser fluence in units of mJ pulse^{-1} cm^{-2}. [f] Obtained from the fits of the kinetics of the CH_3 decay with eq 1. Uncertainties are 1σ (statistical) from the curve fitting. [g] Rate constant of the heterogeneous wall loss obtained from the fits of the kinetics of the CH_3 decay with eq 1. Uncertainties are 1σ (statistical) from the curve fitting. Boron oxide was used as the reactor wall coating. Small negative values of k_w observed in some of the experiments can be attributed to slight imperfections in the relative alignment of the reactor and the photolyzing laser beam.

III. Results

$CH_3 + CH_3$ Reaction: Validation of the Experimental Technique. The values of the rate constant of reaction 7 were determined at 577 K and bath gas densities (mostly helium, balance radical precursors) of 8×10^{16} and 12.0×10^{16} molecules cm^{-3}. The elevated temperature was chosen because at room temperature the rate of the $Cl + CH_4$ reaction is too low ($k = 1 \times 10^{-13}$ cm^3 molecule^{-1} s^{-1})[18,19] to ensure a fast conversion of the photolytically produced Cl atoms into CH_3 radicals; at 577 K this reaction is more than 10 times faster than at 298 K. The exact value of 577 K was chosen to facilitate comparison of the results with those of Slagle and co-workers.[17] The conditions and the results of the experiments in which the reaction between the Cl atoms produced in the photolysis of oxalyl chloride and methane was used to generate methyl radicals are listed in Table 1, together with those of the experiments in which the photolysis of acetone was used as

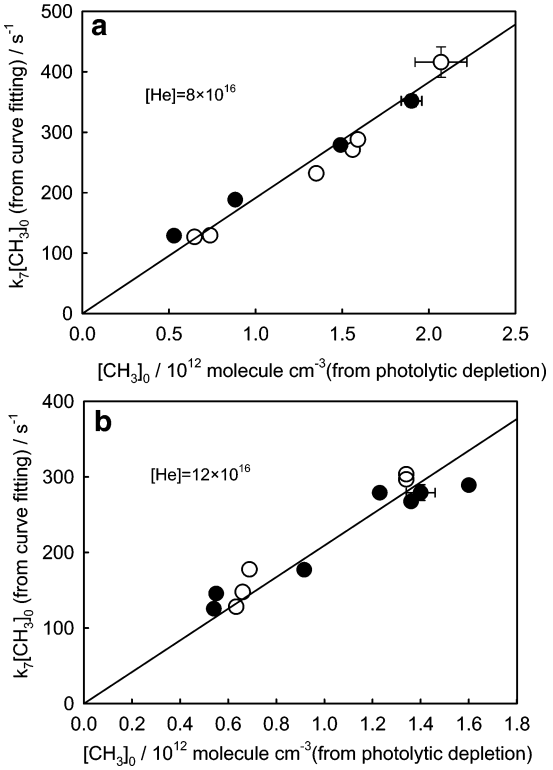

Figure 3. $k_7[CH_3]_0$ vs $[CH_3]_0$ dependences obtained in the experiments on the $CH_3 + CH_3$ reaction at bath gas densities of (a) 8.0×10^{16} and (b) 12.0×10^{16} molecules cm^{-3}. Filled circles represent data points obtained in experiments in which photolysis of acetone was used as a source of methyl radicals; open circles represent data point obtained in experiments in which the combination of reactions 2 and 3 was used to produce methyl radicals. Error bars are shown only for a few representative data points to avoid plot congestion; for actual values of uncertainties, see Table 1.

the source of methyl radicals. The corresponding plots of the $k_r[R]_0$ vs $[R]_0$ dependences are shown in Figure 3, where different symbols indicate experiments performed with different photolytic sources of CH_3. As can be seen from the plots, there is a good convergence between the results obtained using the combination of reactions 2 and 3, on one hand, and the photolysis of acetone (reaction 4), on the other. Thus, the experimental approach based on the use of the photolysis of oxalyl chloride with subsequent conversion of the Cl atoms to hydrocarbon radicals is validated. The values of k_7 obtained in the current study are given in Table 1 and displayed in Figure 4, together with those of Slagle et al.[17] The results of the two experimental studies are in good agreement, providing additional support for the validity of the experimental method used in the current work.

$C_2H_5 + C_2H_5$ Reaction. The values of the rate constant of reaction 1 were determined at room temperature, 400, 600, and 800 K and bath gas densities (mostly helium, balance radical precursors) of 3.0×10^{16} and 12.0×10^{16} molecules cm^{-3} using the combination of reactions 2 and 3 as the photolytic source of C_2H_5. The conditions and results of these experiments are listed in Table 2. Experimental parameters such as the photolyzing laser intensity, the concentrations of oxalyl chloride and ethane, and the reactor wall coating were varied for individual experiments. For each temperature, the values of the $k_r[R]_0$ product obtained under different experimental conditions (including different bath gas densities) are shown on the same $k_r[R]_0$ vs $[R]_0$ plots (Figures 5−8). The rate constant of the ethyl radical self-reaction does not demonstrate any dependence

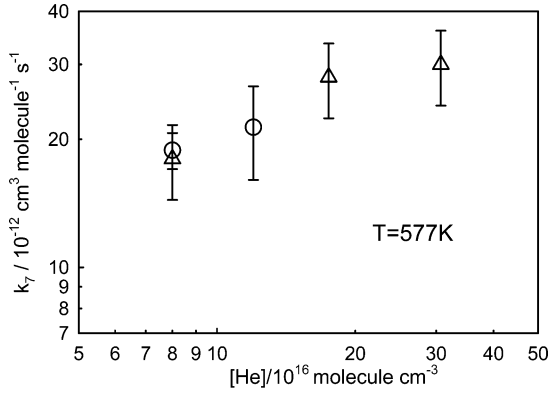

Figure 4. Pressure dependence of the experimentally obtained values of k_7. Circles represent the rate constant values obtained in the current study; triangles represent the results of Slagle et al.[17]

(within the experimental uncertainties) on the parameters varied. Also, no pressure dependence of k_1 can be observed within the experimental uncertainties. Experimental error limits for $k_r[R]_0$ and $[R]_0$ are given in Table 2 for individual data points. The values of k_1 determined from the slopes of the $k_r[R]_0$ vs $[R]_0$ dependences are given in Table 4 for the four experimental temperatures.

The results and conditions of the experiments in which the photolysis of diethyl ketone was used as a source of the ethyl radicals are listed in Table 3, and the corresponding $k_r[R]_0$ vs $[R]_0$ dependences are presented in Figure 9 (two plots display the results obtained at 300 and 800 K). On each plot in Figure 9, the solid lines represent the linear fits of the experimental data, and the dashed lines represent the slopes of the $k_r[R]_0$ vs $[R]_0$ dependences obtained under the same conditions using the combination of reactions 2 and 3 as the photolytic source of the ethyl radicals. As can be seen from the plots, the solid lines lie higher than the dashed lines. Although at room temperature the difference between the values of k_1 obtained using the two photolytic sources of C_2H_5 is relatively minor (17%), at 800 K this difference increases to 53%, which is outside the limits of statistical uncertainties. A potential explanation of the larger value of the slope of the $k_r[R]_0$ vs $[R]_0$ dependence obtained using the photolysis of diethyl ketone is the formation of products other than $CO + 2C_2H_5$ in the act of photolysis (reaction 5). For example, a photolysis channel resulting in the breaking of the C−C bond of the ethyl group in $(C_2H_5)_2CO$ would produce CH_3, C_2H_5, and ketene. A product search revealed formation of C_3H_8, which can be accounted for by the reaction of CH_3 with C_2H_5:

$$CH_3 + C_2H_5 \rightarrow C_3H_8 \qquad (9)$$

The yield of C_3H_8 increased with the temperature: the ratio of the ion signal of C_3H_8 to that of C_4H_{10} (product of the ethyl radical recombination) rose by a factor of 10 upon increasing the temperature from 300 to 800 K. The rate constant of the $CH_3 + C_2H_5$ reaction ($k_9 = 9.8 \times 10^{-11}$ cm^3 $molecule^{-1}$ s^{-1} at room temperature)[22] is significantly larger than that of reaction 1, which can explain the observed faster decay of C_2H_5 in the experiments with the $(C_2H_5)_2CO$ photolysis.

An Arrhenius plot of the rate constant of reaction 1 ($C_2H_5 + C_2H_5$) is shown in Figure 10. The values of k_1 decrease with increasing temperature. This temperature dependence can be

TABLE 2: Conditions and Results of Experiments To Determine k_1

T[a]	[He][b]	[C_2H_6][c]	[$(CClO)_2$][d]	[C_2H_5][e]	I[f]	coating[g]	$k_r[R]_0$[h]	k_w[i]
301	3.0	0.51	6.79	0.93 ± 0.10	38	1	289 ± 11	4.5 ± 1.0
301	3.0	4.55	5.75	0.79 ± 0.09	38	1	231 ± 8	6.0 ± 0.9
301	3.0	4.55	3.94	0.53 ± 0.07	37	1	159 ± 11	3.2 ± 1.6
302	3.0	4.50	1.74	0.19 ± 0.04	30	1	36 ± 4	5.3 ± 3.1
302	3.0	0.51	1.96	0.21 ± 0.04	30	1	47 ± 3	−2.4 ± 2.1
302	3.0	0.51	5.30	0.25 ± 0.06	13	1	111 ± 6	0.4 ± 1.7
302	3.0	0.51	9.97	0.67 ± 0.11	19	1	183 ± 11	0.1 ± 1.7
303	12.0	0.11	4.16	0.55 ± 0.08	37	2	152 ± 4	7.3 ± 0.6
303	12.0	1.18	4.16	0.55 ± 0.08	37	2	155 ± 4	7.9 ± 0.6
303	12.0	1.18	6.63	0.86 ± 0.12	36	2	232 ± 7	9.1 ± 0.7
303	12.0	0.11	6.63	0.86 ± 0.12	36	2	207 ± 7	7.6 ± 0.7
303	12.0	0.11	9.84	1.11 ± 0.25	31	2	286 ± 10	7.2 ± 0.7
303	12.0	1.20	9.85	1.11 ± 0.25	31	2	316 ± 11	8.0 ± 0.7
303	12.0	5.74	9.85	1.11 ± 0.25	31	2	323 ± 12	9.7 ± 0.7
303	12.0	5.74	2.25	0.28 ± 0.05	34	2	67 ± 4	7.3 ± 1.4
303	12.0	1.17	2.25	0.28 ± 0.05	34	2	70 ± 3	5.9 ± 0.1
400	3.0	0.55	4.66	0.60 ± 0.10	40	2	182 ± 10	4.9 ± 2.5
400	3.0	4.70	4.04	0.48 ± 0.12	37	2	131 ± 9	8.9 ± 3.0
400	3.0	4.70	5.68	0.63 ± 0.09	34	2	225 ± 15	1.0 ± 2.8
400	3.0	4.70	10.0	1.40 ± 0.28	44	2	383 ± 27	9.6 ± 2.4
400	3.0	0.54	11.3	1.59 ± 0.32	44	2	468 ± 31	3.6 ± 2.1
400	12.0	0.49	2.18	0.23 ± 0.04	33	2	116 ± 6	−0.5 ± 1.3
400	12.0	0.49	4.85	0.68 ± 0.14	45	2	206 ± 11	2.1 ± 1.2
400	12.0	0.49	1.04	1.65 ± 0.15	50	2	396 ± 31	4.6 ± 1.3
400	12.0	0.49	7.52	1.00 ± 0.13	42	2	304 ± 18	2.5 ± 1.0
400	12.0	5.32	6.94	0.96 ± 0.14	43	2	294 ± 18	1.8 ± 1.1
400	12.0	5.32	4.34	0.56 ± 0.10	40	2	170 ± 9	2.6 ± 1.2
600	12.0	0.47	2.05	0.25 ± 0.10	23	3	61 ± 6	18.9±4.3
600	12.0	0.47	5.61	1.09 ± 0.22	37	3	228 ± 11	29.0 ± 1.6
600	12.0	4.90	3.50	0.73 ± 0.33	40	3	137 ± 15	27.2 ± 3.7
600	12.0	0.48	2.94	0.58 ± 0.10	38	3	120 ± 5	33.0 ± 1.6
600	12.0	0.48	12.2	2.24 ± 0.19	35	3	504 ± 22	31.7 ± 1.1
600	12.0	4.37	9.40	2.30 ± 0.17	47	3	449 ± 27	26.4 ± 1.6
600	12.0	4.37	5.68	1.36 ± 0.08	46	3	319 ± 14	21.0 ± 1.4
600	12.0	4.37	8.02	1.85 ± 0.13	44	3	499 ± 33	21.3 ± 1.7
600	12.0	0.44	7.50	1.50 ± 0.27	38	3	273 ± 13	32.1 ± 1.5
600	12.0	0.44	7.98	1.59 ± 0.19	38	3	275 ± 10	35.5 ± 1.2
600	12.0	5.32	10.6	1.71 ± 0.17	31	3	384 ± 23	22.6 ± 1.7
800	3.0	1.01	23.0	3.25 ± 0.54	28	1	663 ± 59	24.7 ± 3.7
800	3.0	1.03	20.5	4.87 ± 0.57	47	1	861 ± 103	15.5 ± 4.5
800	3.0	4.52	20.7	4.92 ± 0.63	47	1	806 ± 73	5.7 ± 3.6
800	3.0	1.03	18.6	4.01 ± 0.65	42	1	469 ± 40	7.5 ± 4.5
800	3.0	1.10	22.0	3.79 ± 0.58	34	1	709 ± 64	2.2 ± 3.9
800	3.0	1.10	22.0	3.79 ± 0.58	34	1	631 ± 43	1.5 ± 3.2
800	3.0	10.80	23.1	4.54 ± 0.45	39	1	916 ± 93	0.0 ± 4.0
800	3.0	10.80	23.1	4.54 ± 0.45	39	1	841 ± 97	4.0 ± 4.5
800	3.0	1.03	19.9	2.87 ± 0.45	28	1	480 ± 33	19.9 ± 3.5
800	3.0	1.03	19.9	2.87 ± 0.45	28	1	487 ± 36	22.4 ± 3.7
800	3.0	1.03	28.5	3.84 ± 0.39	26	1	696 ±	16.6 ± 4.4
800	3.0	1.03	28.5	3.84 ± 0.39	26	1	711 ± 73	11.6 ± 4.3
800	12.0	1.13	6.28	0.99 ± 0.15	31	1	180 ± 19	13.1 ± 6.8
800	12.0	1.23	9.88	1.54 ± 0.24	31	1	214 ± 23	33.8 ± 6.4
800	12.0	1.24	8.02	1.47 ± 0.14	36	1	224 ± 28	22.3 ± 7.6
800	12.0	1.24	6.11	1.08 ± 0.14	35	1	141 ± 17	33.6 ± 7.4
800	12.0	0.28	6.86	1.19 ± 0.10	34	1	156 ± 19	45.3 ± 7.0
800	12.0	0.28	4.85	0.83 ± 0.14	34	1	119 ± 14	24.1 ± 7.0
800	12.0	0.31	11.0	2.05 ± 0.36	37	1	240 ± 26	42.3 ± 6.3
800	12.0	0.35	9.74	1.62 ± 0.17	33	1	243 ± 32	29.4 ± 7.7
800	12.0	2.77	9.78	1.60 ± 0.23	32	1	268 ± 39	20.5 ± 8.8
800	12.0	2.77	14.2	2.26 ± 0.33	31	1	290 ± 33	23.2 ± 6.7
800	12.0	3.22	24.5	5.48 ± 0.76	44	1	776 ± 88	20.1 ± 4.4
800	12.0	10.00	22.6	3.71 ± 0.43	32	1	542 ± 31	21.0 ± 3.0
800	12.0	10.00	22.6	3.71 ± 0.43	32	1	589 ± 29	18.0 ± 2.2
800	12.0	10.00	31.6	5.06 ± 0.66	31	1	811 ± 53	14.0 ± 2.5
800	12.0	10.00	31.6	5.06 ± 0.66	31	1	795 ± 47	17.0 ± 2.3

[a] Temperature in units of K. [b] Concentration of the bath gas (mostly helium, balance radical precursors) in units of 10^{16} atoms cm^{-3}. [c] In units of 10^{15} molecules cm^{-3}. [d] In units of 10^{13} molecules cm^{-3}. [e] Nascent concentration of ethyl radicals in units of 10^{13} molecules cm^{-3}, determined from the photolytic depletion of oxalyl chloride. [f] Estimated laser fluence in units of mJ $pulse^{-1}$ cm^{-2}. [g] Reactor wall coating: 1, boron oxide; 2, halocarbon wax; 3, poly(dimethylsiloxane). [h] Obtained from the fits of the kinetics of the C_2H_5 decay with eq 1. Uncertainties are 1σ (statistical) from the curve fitting. [i] Rate constant of the heterogeneous wall loss obtained from fits of the kinetics of the C_2H_5 decay with eq 1. Uncertainties are 1σ (statistical) from the curve fitting. Small negative values of k_w observed in some of the experiments can be attributed to slight imperfections in the relative alignment of the reactor and the photolyzing laser beam.

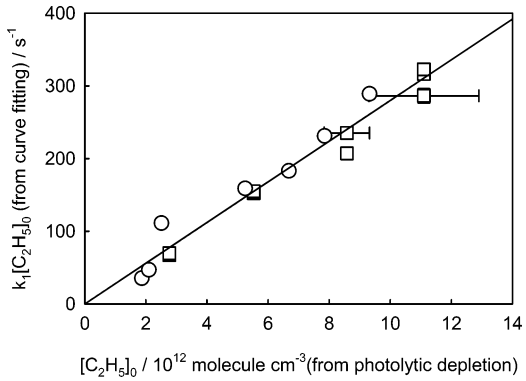

Figure 5. $k_1[C_2H_5]_0$ vs $[C_2H_5]_0$ dependence obtained in the study of reaction 1 at room temperature. Circles, bath gas density = 12.0×10^{16} molecules cm^{-3}; squares, bath gas density = 3.0×10^{16} molecules cm^{-3}. Error bars are shown only for a few representative data points to avoid plot congestion; for actual values of uncertainties, see Table 2.

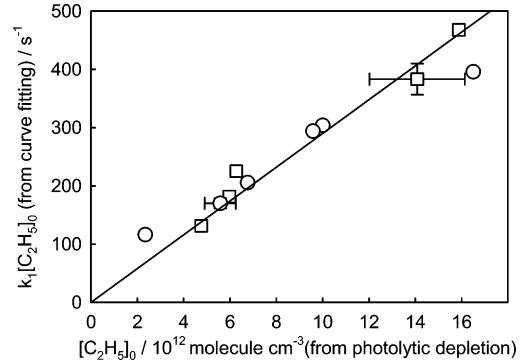

Figure 6. $k_1[C_2H_5]_0$ vs $[C_2H_5]_0$ dependence obtained in the study of reaction 1 at 400 K. Circles, bath gas density = 12.0×10^{16} molecules cm^{-3}; squares, bath gas density = 3.0×10^{16} molecules cm^{-3}. Error bars are shown only for a few representative data points to avoid plot congestion; for actual values of uncertainties, see Table 2.

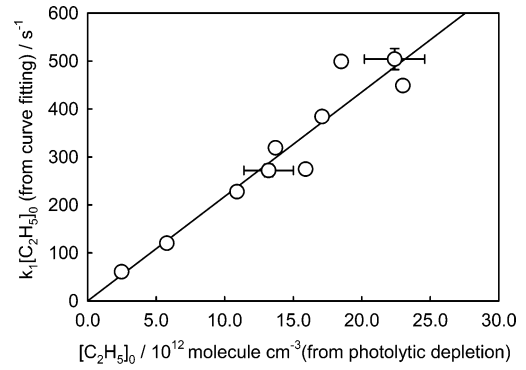

Figure 7. $k_1[C_2H_5]_0$ vs $[C_2H_5]_0$ dependence obtained in the study of reaction 1 at 600 K. Error bars are shown only for a few representative data points to avoid plot congestion; for actual values of uncertainties, see Table 2.

represented with a parametric fit given by the expression

$$k_1 = (4.36 \times 10^{-5}) T^{-2.08} \exp\left(-\frac{718\ \mathrm{K}}{T}\right) \mathrm{cm^3\ molecule^{-1}\ s^{-1}} \quad \text{(II)}$$

The disproportionation-to-recombination branching ratio of reaction 1 was determined at two temperatures (297 and 400 K) and the bath gas density of 12.0×10^{16} molecule cm^{-3}. The conditions and the results of these experiments are presented in Table 5.

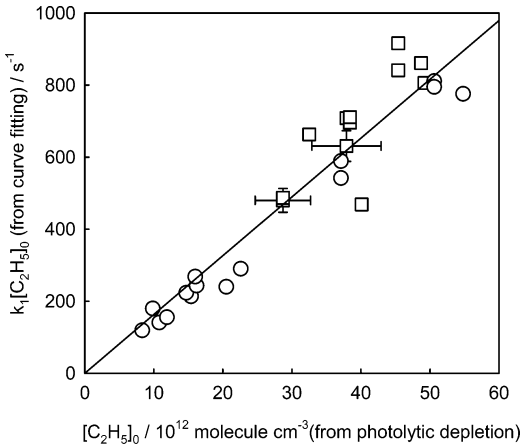

Figure 8. $k_1[C_2H_5]_0$ vs $[C_2H_5]_0$ dependence obtained in the study of reaction 1 at 800 K. Circles, bath gas density = 12.0×10^{16} molecules cm^{-3}; squares, bath gas density = 3.0×10^{16} molecules cm^{-3}. Error bars are shown only for a few representative data points to avoid plot congestion; for actual values of uncertainties, see Table 2.

TABLE 3: Conditions and Results of Experiments with Photolysis of $(C_2H_5)_2CO$ as the Ethyl Radical Source

T[a]	He[b]	$[(C_2H_5)_2CO]$[c]	$[C_2H_5]$[d]	I[e]	$k_1[R]_0$[f]	k_w[g]
296	12.0	37.0	0.32 ± 0.03	38	92 ± 4	2.6 ± 1.4
296	12.0	14.3	1.01 ± 0.06	29	335 ± 2	-0.9 ± 1.1
304	12.0	4.92	0.36 ± 0.04	30	109 ± 3	5.4 ± 0.8
304	12.0	10.7	0.73 ± 0.05	28	240 ± 5	2.0 ± 0.6
800	3	7.17	0.72 ± 0.06	38	212 ± 13	23.6 ± 4.1
800	3	5.56	0.53 ± 0.05	38	128 ± 10	23.6 ± 4.6
800	3	11.2	1.01 ± 0.08	28	258 ± 18	26.2 ± 4.2
800	3	19.2	1.60 ± 0.13	28	386 ± 34	26.7 ± 4.8

[a] Temperature in units of K. [b] Concentration of the bath gas (mostly helium, balance radical precursors) in units of 10^{16} atoms cm^{-3}. [c] In units of 10^{14} molecules cm^{-3}. [d] Nascent concentration of ethyl radicals in units of 10^{13} molecules cm^{-3}, determined from the photolytic depletion of diethyl ketone. [e] Estimated laser fluence in units of mJ $pulse^{-1}$ cm^{-2}. [f] Obtained from the fits of the kinetics of the C_2H_5 decay with eq 1. Uncertainties are 1σ (statistical) from the curve fitting. [h] Rate constant of the heterogeneous wall loss obtained from fits of the kinetics of the C_2H_5 decay with eq 1. Uncertainties are 1σ (statistical) from the curve fitting. Boron oxide was used as the reactor wall coating.

IV. Discussion

Falloff Effects. Experimental values of the rate constant of reaction 1 were obtained at low bath gas pressures, where falloff can potentially be of importance. The extent of pressure effects on the rate of C_2H_5 radical self-reaction was evaluated with the method used by us earlier in the studies of the reactions of propargyl, allyl, ethyl, *n*-propyl, and *n*-butyl radicals with CH_3.[22,23] Approximate values of the microscopic energy-dependent rate constants for decomposition of the C_4H_{10} adduct were obtained using a method based on the inverse Laplace transform of the temperature dependence of the high-pressure-limit recombination rate.[23] Calculations of the falloff corrections performed in the current work exactly follow the iterative procedure of master equation modeling of refs 22 and 23. The models (including the properties of the collisional energy transfer) and the heats of formation of the species involved (C_2H_5 and C_4H_{10}) are the same as those used in ref 22 for the reactions $C_2H_5 + CH_3 \rightarrow C_3H_8$ and $n\text{-}C_3H_7 + CH_3 \rightarrow C_4H_{10}$. The existence of the disproportionation channel (1b) of reaction 1 was taken into account; the disproportionation-to-combination ratio was taken as equal to 0.14,[3,4] as supported by the results of the current experimental study. The presence of polyatomic species (oxalyl chloride and ethane) in the bath gas was also taken into account. The values of $\langle \Delta E \rangle_{\mathrm{down}}$ (average energy

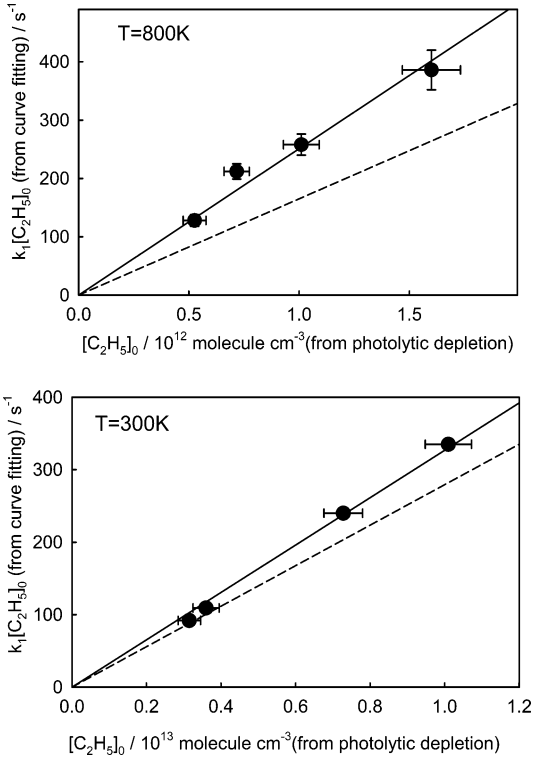

Figure 9. Comparison between the $k_1[C_2H_5]_0$ vs $[C_2H_5]_0$ dependences obtained using different radical sources. Circles represent the values of $k_1[C_2H_5]_0$ obtained in experiments that used 193-nm photolysis of diethyl ketone as a source of ethyl radicals; solid lines are fits through these data. Dashed lines show the slopes of the $k_1[C_2H_5]_0$ vs $[C_2H_5]_0$ dependences obtained in experiments with the combination of reactions 2 and 3 used as a source of ethyl radicals.

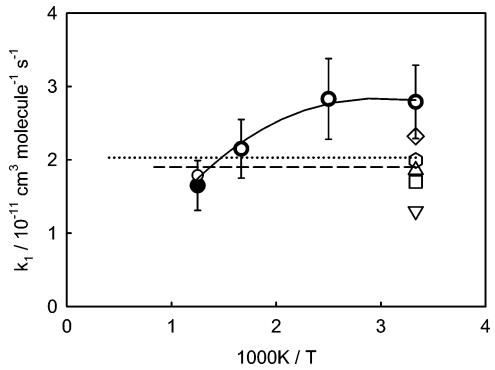

Figure 10. Temperature dependence of the experimentally obtained values of k_1 (filled circles) and the extrapolated values of k_1^∞ (open smaller circles). The near coincidence of the filled and the open circles (open small circles are superimposed on the larger filled circles) demonstrates that reaction 1 is at the high-pressure limit under the conditions of all experiments, except for an 8% deviation at 800 K. The inverted triangle, triangle, square, diamond, and hexagon represent the values of k_1 reported in refs 6, 7, 8, 9, and 10, respectively. The solid line represents the fit of eq III. The dashed and the dotted lines represent the k_1 values recommended in reviews by Baulch et al.[4] and Tsang and Hampson[1], respectively.

transferred per deactivating collision with the bath gas)[24,25] used for the collisions between C_4H_{10} and these polyatomic species was taken as 2 times larger that the value for the $C_4H_{10}-He$ pair.

It was found that reaction 1 is very close to the high-pressure limit under all conditions of the current experimental study. The falloff factor (k_1/k_1^∞) is unity under all experimental conditions except for the highest temperature used, 800 K, where it is equal to 0.92. These evaluated falloff factors and appropriate corrections for the rate constants are given in Table 4. The uncertainty of extrapolation to the high-pressure limit was evaluated following the procedure of refs 22 and 23. The overall uncertainty factors given in Table 4 for the high-pressure-limit rate constant values represent combinations of the experimental uncertainties and those due to falloff extrapolation.

TABLE 4: Temperature Dependence of the Rate Constant of Reaction 1

T/K	[M][a]	k_1[b]	k_1/k_1^∞ [c]	k_1^∞ [d]	*F* [e]
300	3, 12.0	2.79 ± 0.49	1.0	2.79	1.18
400	3, 12.0	2.83 ± 0.46	1.0	2.83	1.16
600	12.0	2.15 ± 0.27	1.0	2.15	1.14
800	3, 12.0	1.65 ± 0.22	0.92	1.77	1.22

[a] Concentration of the bath gas (mostly helium, balance precursors) in units of 10^{16} molecules cm^{-3}. [b] Rate constant of reaction 1 in units of 10^{-11} molecules cm^{-3} s^{-1}. [c] Calculated falloff correction factor (see ref 22). [d] k_1^∞ obtained by dividing the experimental k_1 values by the calculated k_1/k_1^∞ correction factor. [e] *F* is the uncertainty factor of k_1^∞ (i.e., upper and lower limiting values of k_1^∞ can be obtained by multiplying or dividing the optimum value by *F*). For 800 K, *F* includes the estimated uncertainty of extrapolation to the high-pressure limit and the experimental uncertainty. For all other measurements, *F* includes only the experimental uncertainty.

TABLE 5: Product Branching Ratios

T/K	[M][a]	$[C_2H_6]$[b]	$[(CClO)_2]$[c]	*I* [d]	k_{1b}/k_{1a}
297	12.0	1.15	5.63	19	0.12 ± 0.07
297	12.0	1.13	4.34	11	0.18 ± 0.09
400	12.0	1.21	6.09	23	0.18 ± 0.08

[a] Concentration of the bath gas (mostly helium, balance radical precursors) in units of 10^{16} molecules cm^{-3}. [b] In units of 10^{16} molecules cm^{-3}. [c] In units of 10^{14} molecules cm^{-3}. [d] Estimated laser fluence in units of mJ $pulse^{-1}$ cm^{-2}.

The temperature dependence of the high-pressure-limit rate constant of reaction 1 can be represented with the following expression:

$$k_1 = (2.29 \times 10^{-6}) T^{-1.66} \exp\left(-\frac{552\ \mathrm{K}}{T}\right) \mathrm{cm^3\ molecule^{-1}\ s^{-1}} \quad \text{(III)}$$

Rate Constant Values. This work presents the first direct real-time experimental determination of the rate constant of the $C_2H_5 + C_2H_5$ reaction (k_1) as a function of temperature (301−800 K). The room-temperature values of the rate constant of reaction 1 reported in earlier studies[6−10] are shown in Figure 10, together with the values obtained in the current study and the values recommended in two reviews (refs 1 and 4). As can be seen from the plot, the room-temperature value of k_1 obtained in the current work ($(2.79 \pm 0.49) \times 10^{-11}$ cm^3 $molecule^{-1}$ s^{-1}) is higher than the results of previous determinations; however, the results of Adachi et al.[9] ($(2.32 \pm 0.45) \times 10^{-11}$ cm^3 $molecule^{-1}$ s^{-1}) and Atkinson and Hudgens[10] ($(1.99 \pm 0.44) \times 10^{-11}$ cm^3 $molecule^{-1}$ s^{-1}) agree with those of the current study within the combined experimental uncertainties. The values reported by Parkes and Quinn[6] ($(1.5 \pm 0.4) \times 10^{-11}$ cm^3 $molecule^{-1}$ s^{-1}), Arthur[7] ($(1.86 \pm 0.32) \times 10^{-11}$ cm^3 $molecule^{-1}$ s^{-1}), and Anastasi and Arthur[8] ($(1.69 \pm 0.15) \times 10^{-11}$ cm^3 $molecule^{-1}$ s^{-1}) are significantly lower than those of the current work, with the differences being larger than the combined error limits. The only previous study of the ethyl radical self-reaction at higher temperatures (373 K) was reported by Arthur,[7] who did not observe any temperature dependence of the rate constant in the 300−373 K temperature range. The rate constant of reaction 1 obtained in the current work demonstrates a negative temperature dependence; the room-

temperature value is higher than that recommended by the reviews of Tsang and Hampson[1] (2.03×10^{-11} cm^3 molecule^{-1} s^{-1}) and Baulch et al.[4] (1.9×10^{-11} cm^3 molecule^{-1} s^{-1}); however, at 800 K the experimental rate constant value is lower than these recommendations.

Earlier studies in which the values of k_1 were obtained by indirect methods, such as fitting of complex kinetic mechanisms, were reviewed in refs 1, 3, and 4. These studies are not discussed here because their results relied on estimated rate constants and/or assumed knowledge of the mechanisms of complex kinetic systems. In 1976, Parkes and Quinn[6] used molecular modulation spectrometry to determine the rate constant of reaction 1. In their experiments, ethyl radicals were created by square-wave photolysis of a radical precursor (diazoethane) and detected by absorption spectroscopy. The value of the rate constant was derived from the in-phase and the in-quadrature absorption signals of the radicals. The method relies on the knowledge of the absorption cross section of ethyl radicals, which was determined in separate experiments. Parkes and Quinn reported low sensitivity toward C_2H_5 in their experiments.

Adachi, Basco, and James[9] studied ethyl radical self-reactions by means of flash photolysis/UV absorption spectroscopy. Ethyl radicals were produced by the photolysis of azoethane in an atmosphere of nitrogen. Radical decay was monitored in real time by UV absorption. These experiments also relied on knowledge of the absorption cross section of the ethyl radicals. The value of the absorption cross section determined at the wavelength of 247 nm in their study is higher than that reported by Parkes and Quinn at 248 nm (the authors report the spectra of ethyl radical as a broad peak with the maximum absorption between 242 and 252 nm) but coincides (within experimental uncertainties) with that used in a later study by Anastasi and Arthur at 250 nm.[8] Although Adachi et al. reported that they increased the sensitivity of their apparatus toward C_2H_5 almost 10-fold (relative to their previous experimental setup), they stated that this increased sensitivity was still low and that concentrations of ethyl radicals just above the detection limits of their apparatus were used in the experiments.

Arthur[7] and Anastasi and Arthur[8] used molecular modulation spectroscopy to study the ethyl radical self-reaction. The experimental technique used in their study was similar to that used by Parkes and Quinn. Ethyl radicals were obtained in the photolysis of diazoethane in an atmosphere of nitrogen. These authors also reported a low sensitivity toward ethyl radicals.

A recent study by Atkinson and Hudgens[10] reported a room-temperature value of the rate constant of reaction 1 ($(1.99 \pm 0.44) \times 10^{-11}$ molecule^{-1} s^{-1}) that is in agreement with the values obtained by molecular modulation spectroscopy and, within combined experimental uncertainties, with the value determined in the current work. The technique of ultraviolet cavity ring-down spectroscopy allowed the authors to detect relatively low concentrations of ethyl radicals (reported detection limit $\sim 10^{12}$ molecule cm^{-3}). Ethyl radicals were created by the photolysis of Cl_2, followed by a rapid reaction of the chlorine atoms with ethane. As was acknowledged by the authors, ethyl radicals rapidly reacted with the unphotolyzed Cl_2. However, the authors assumed that, since the thus-produced Cl atoms were rapidly converted to C_2H_5 by reaction with ethane, the overall combination of the $C_2H_5 + Cl_2$ and the $Cl + C_2H_6$ reactions should have no influence on the determination of the rate constant of the ethyl radical self-reaction. The $C_2H_5 + Cl_2$ reaction is fast[26] ($k = 2.10 \times 10^{-11}$ cm^3 molecule^{-1} s^{-1}), which, under the experimental conditions ($[Cl_2] \approx (2.5-12) \times 10^{15}$ and $[C_2H_6] \approx 6 \times 10^{15}$ molecules cm^{-3}) employed in the study of ref 10, can be expected to lead to a fast chain reaction with a characteristic turnover time of only $\sim 10^{-5}$ s (more than 3 orders of magnitude faster than the typical time of the kinetics of C_2H_5 decay due to reaction 1). In their analysis of the experimental data, the authors of ref 10 did not account for this chain reaction and for the pseudo-steady-state concentration of Cl atoms created by it, which can possibly explain the differences between the room-temperature values of k_1 obtained in the current study and in ref 10.

The experimental apparatus employed in the current study has a detection limit toward ethyl radicals of approximately 10^9 molecules cm^{-3}. The concentrations of radicals used in this study were always at least 3 orders of magnitude larger than the detection limit. This high sensitivity of the apparatus, combined with the well-characterized photolytic source of the radicals, enabled the determination of the rate constant of ethyl radical self-reaction in direct time-resolved experiments over a wide range of temperatures (301−800 K).

Channel Branching. The disproportionation-to-recombination ratio of reaction 1 has been determined previously by a large number of independent groups (see, for example, the review in ref 3), most of which employed chromatographic product analysis to measure the ratio of disproportionation to recombination channels. The k_{1b}/k_{1a} ratios determined in the current study at 297 and 400 K (Table 5) are in agreement with the value of 0.14 resulting from these earlier studies.[3,4] A combination of the low sensitivity of the apparatus employed in the current study toward ethylene and the strong ion fragmentation signal at mass 28 from butane and ethane resulted in relatively large uncertainties in the experimental k_{1b}/k_{1a} ratio and prevented us from determining the channel branching ratio at higher temperatures.

Photolysis of Diethyl Ketone. Photolysis of ketones has been widely used as a convenient photolytic source of radicals in studies of reaction kinetics and product analysis. In a number of studies, distribution of photolysis products has been determined (e.g., refs 16 and 27). Usually, 193-nm photolysis of an $R^1C(O)R^2$ ketone in the gas phase yields $R^1 + R^2 + CO$ as the products of the major channel. The well-documented dominance of such product channels in the photolysis of acetone[16] and methyl vinyl ketone[27] enabled a number of kinetic studies in which 193-nm photolysis of these ketones was used to create known concentrations of radicals of interest. In this respect, it is interesting to investigate the 193-nm photolysis of diethyl ketone (reaction 5) in order to assess its suitability as a quantitatively characterized source of C_2H_5 radicals for kinetic studies. In the current study, attempts were made to use reaction 5 as an alternative source of ethyl radicals for the study of the C_2H_5 self-reaction. It was demonstrated that, if photolytic depletion of diethyl ketone was used to evaluate the nascent concentrations of C_2H_5 under the assumption that the channel producing $2C_2H_5 + CO$ (5a) is the only important pathway of the photolysis, then the apparent values of the rate constant of the ethyl radical self-reaction are larger than those obtained with a better characterized source of ethyl radicals (reactions 2 and 3). Although at room temperature the difference in the slopes of the $k_r[R]_0$ vs $[R]_0$ dependences obtained using reaction 5 and a combination of reactions 2 and 3 was only minor and fell within the envelope of data scatter, at 800 K this difference was much more pronounced. Furthermore, formation of C_3H_8 was observed when diethyl ketone was used as a photolytic

source of C_2H_5, indicating the likely presence of a second route of photolysis,

$$(C_2H_5)_2CO \xrightarrow{193\ nm} CH_3 + CH_2CO + C_2H_5 \qquad (5c)$$

followed by recombination of CH_3 and C_2H_5,

$$CH_3 + C_2H_5 \rightarrow C_3H_8 \qquad (9)$$

The yield of C_3H_8 increased with temperature: the ratio of the ion signals of C_3H_8 and C_4H_{10} increased by a factor of 10 from 300 to 800 K. The rate constant of reaction 9 is 2−3.5 times larger[22] than that of reaction 1 in the 300−800 K temperature range, which explains the faster decays of C_2H_5 observed in the experiments with diethyl ketone and the increase of the differences with temperature.

These findings are in general agreement with the results of Fischer and Mains,[28] who studied the temperature dependence of the distribution of products of flash photolysis (210−450 nm) of diethyl ketone using gas chromatography. These authors also detected a higher yield of propane at higher temperatures and suggested that production of propane should become dominant at lower wavelengths of the photolyzing light. Due to limitations of their experimental apparatus (xenon lamps were used as the light source), the authors could not perform experiments at wavelengths shorter than 210 nm. The results of the experiments conducted in the current study and those of Fischer and Mains suggest that, although formation of two ethyl radicals and CO is likely to be the dominant channel of the 193-nm photolysis of diethyl ketone at room temperature, at higher temperatures formation of CH_3 also becomes important.

Acknowledgment. This research was supported by the Division of Chemical Sciences, Office of Basic Energy Sciences, Office of Energy Research, U.S. Department of Energy, under Grant No. DE/FG02-98ER14463.

References and Notes

(1) Tsang, W.; Hampson, R. F. *J. Phys. Chem. Ref. Data* **1986**, *15*, 1087.

(2) Warnatz, J.; Mass, U.; Dibble, R. W. *Combustion: Physical and Chemical Fundamentals, Modeling and Simulation, Experiments, Pollutant Formation*; Springer: Berlin, Heidelberg, New York, 1996.

(3) Kerr, J. A. In *CRC Handbook of Bimolecular and Termolecular Gas Reactions.*; Moss, S. J., Asst. Ed.; CRC Press: Boca Raton, FL, 1981; Vol. 2.

(4) Baulch, D. L.; Cobos, C. J.; Cox, R. A.; Esser, C.; Frank, P.; Just, Th.; Kerr, J. A.; Pilling, M. J.; Troe, J.; Walker, R. W.; Warnatz, J. *J. Phys. Chem. Ref. Data* **1992**, *21*, 411.

(5) Shepp, A.; Kutschke, K. O. *J. Chem. Phys.* **1957**, *26*, 1020.

(6) Parkes, D. A.; Quinn, C. P. *J. Chem. Soc., Faraday Trans. 1* **1976**, *72*, 1952.

(7) Arthur, N. L. *J. Chem. Soc., Faraday Trans. 2* **1986**, *82*, 1057.

(8) Anastasi, C.; Arthur, N. L. *J. Chem. Soc., Faraday Trans. 2* **1987**, *83*, 277.

(9) Adachi, H.; Basco, N.; James, D. G. L. *Int. J. Chem. Kinet.* **1979**, *11*, 995.

(10) Atkinson, D. B.; Hudgens, J. W. *J. Phys. Chem. A* **1997**, *101*, 3901.

(11) Baklanov, A. V.; Krasnoperov, L. N. *J. Phys. Chem. A* **2001**, *105*, 97.

(12) Baklanov, A. V.; Krasnoperov, L. N. *J. Phys. Chem. A* **2001**, *105*, 4917.

(13) Slagle, I. R.; Gutman, D. *J. Am. Chem. Soc.* **1985**, *107*, 5342.

(14) Niiranen, J. T.; Gutman, D.; Krasnoperov, L. N. *J. Phys. Chem.* **1992**, *96*, 5881.

(15) Nicovich, J. M.; Kreutter, K. D.; Wine, P. H. *J. Chem. Phys.* **1990**, *92*, 3539.

(16) Lightfoot, P. D.; Kirwan, S. P.; Pilling, M. J. *J. Phys. Chem.* **1988**, *92*, 4938.

(17) Slagle, I. R.; Gutman, D.; Davies, J. W.; Pilling, M. J. *J. Phys. Chem.* **1988**, *92*, 2455.

(18) Bryukov, M. G.; Slagle, I. R.; Knyazev, V. D. *J. Phys. Chem. A* **2002**, *106*, 10532.

(19) Pilgrim, J. S.; McIlroy, A.; Taatjes, C. A. *J. Phys. Chem. A* **1997**, *101*, 1873.

(20) Seakins, P. W.; Woodbridge, E. L.; Leone, S. R. *J. Phys. Chem.* **1993**, *97*, 5633.

(21) Bevington, P. R. *Data Reduction and Error Analysis for the Physical Sciences*; McGraw-Hill: New York, 1969.

(22) Knyazev, V. D.; Slagle, I. R. *J. Phys. Chem. A* **2001**, *105*, 6490.

(23) Knyazev, V. D.; Slagle, I. R. *J. Phys. Chem. A* **2001**, *105*, 3196.

(24) Gilbert, R. G.; Smith, S. C. *Theory of Unimolecular and Recombination Reactions*; Blackwell: Oxford, 1990.

(25) Rabinovitch, B. S.; Tardy, D. C. *J. Chem. Phys.* **1966**, *45*, 3720.

(26) Timonen, R. S.; Gutman, D. *J. Phys. Chem.* **1986**, *90*, 2987.

(27) Fahr, A.; Laufer, A. H. *J. Phys. Chem.* **1988**, *92*, 7229.

(28) Fischer, L. C.; Mains, G. J. *J. Phys. Chem.* **1964**, *68*, 188.